AN ANALYSIS OF PRESOLAR SIC X GRAINS AND MAINSTREAM GRAINS USING TRANSMISSION ELECTRON MICROSCOPY. K. M. Hynes, S. Amari, T. K. Croat, A. F. Mertz, and T. J. Bernatowicz, Laboratory for Space Sciences and Department of Physics, Washington University, St. Louis, MO 63130, USA, kmhynes@wustl.edu.

Introduction: Most presolar SiC grains (>90%) originated in the outflows of asymptotic giant branch (AGB) stars and typically have enrichments in ^{13}C, ^{14}N, and $^{29,30}Si$ [1]. However, only ~1% of all presolar SiC grains show evidence of a supernova (SN) origin [2]. These grains, known as SiC X grains, are isotopically very distinct from mainstream grains. Based on their isotopic composition, namely large ^{28}Si excesses, as well as the inferred initial presence of radioactive isotopes like ^{26}Al, ^{44}Ti [3], and ^{49}V [4], X grains are thought to have condensed in SN outflows. While isotopic studies have been performed on hundreds of X grains and thousands of mainstream grains, transmission electron microscopy (TEM) studies are limited. Over 500 small SiC grains (~0.5 µm in diameter) were analyzed in the TEM, but most of these grains were mainstream SiC with very limited isotopic data available [5]. Correlated isotopic and microstructural information has been obtained for only a few grains [6, 7]. Here we present results on seven SiC X grains and two mainstream grains from the same size fraction in order to compare the microstructural results of formation in two very different astrophysical environments.

Experimental: SiC X grains and mainstream grains from the KJG fraction (~3 µm in diameter [8]) of the Murchison meteorite were located by ion imaging with the IMS-3f. Their C and Si isotopic ratios were subsequently measured in the NanoSIMS to confirm their origin. Seven typical X grains and two typical mainstream grains were removed from the Au NanoSIMS mount, placed into resin, and then sliced into 70 nm sections with a diamond ultramicrotome. The slices were studied in a JEOL 2000FX TEM.

Results and Discussion: Silicon isotopic data for the nine SiC grains are plotted in Figure 1. All of the X grains show large ^{28}Si excesses and are more depleted in ^{30}Si than ^{29}Si. The X grains in this study all plot near a line of slope 0.67, which is the line defined by most X grains on a Si three-isotope plot [9]. The mainstream grains in this study plot near the line defined by mainstream grains (slope 1.37) [10]. The C and N isotopes for all the grains in this study also lie within the previously observed ranges.

Energy Dispersive X-ray Spectrometer (EDXS) measurements were made on all the grains. The X grains showed Si and C, as well as varying amounts of Al and Mg. Only one X grain did not contain measurable amounts of Al or Mg, with upper limits near 0.7 and 0.2 atomic %, respectively. A second X grain had Al, but no quantifiable Mg. The remaining five X grains had Al and Mg concentrations that ranged from 1.4 – 6.5 and 0.6 – 5.0 atomic %, respectively. The Mg/Al ratios were quite large, ranging from 0.44 – 0.74. In comparison, the mainstream grains contained a similar amount of Al, but no measurable Mg. Magnesium, unlike Al, does not typically condense into SiC during its formation. Since very little Mg is measured in mainstream grains (Mg/Al < 0.05 [11]), the high Mg/Al ratios are likely due to the incorporation of live radioactive ^{26}Al into the X grain during formation and its subsequent decay into ^{26}Mg. Therefore, the elemental Mg/Al ratios obtained from EDXS are roughly analogous to $^{26}Al/^{27}Al$ ratios and are consistent with isotopic measurements made on other SiC X grains [9].

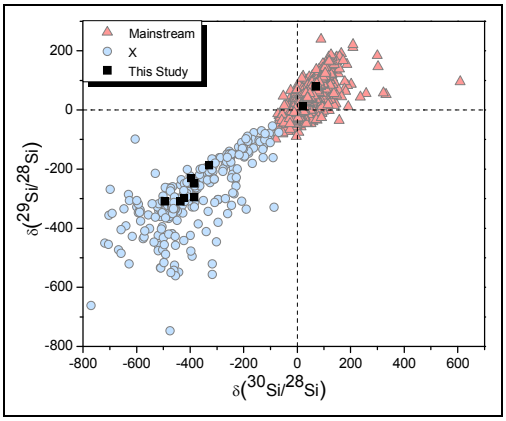

Figure 1. Silicon isotopic ratios of SiC selected for TEM study (black squares), compared to mainstream and X grain presolar data from references in [12]. All ratios are expressed as permil deviations from the solar ratios (δ values).

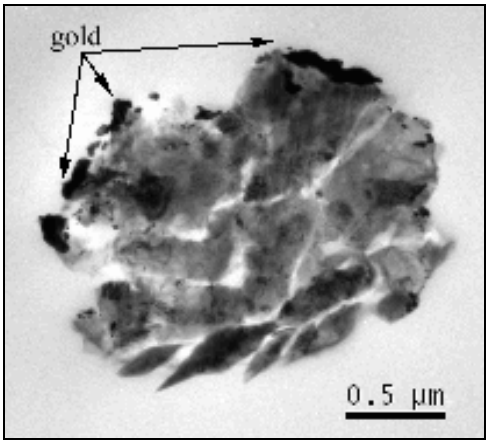

Figure 2. Bright field (BF) TEM image of an ultramicrotome slice of a KJG SiC X grain. Because SiC is so hard, the grain shatters when sliced, but individual crystal domains are visible within the fragments. The black areas at the top of the slice are Au deposits from NanoSIMS analysis.

The slices of the grains had an average diameter of 2.3 µm. Figure 2 shows a typical SiC X grain cross-section after ultramicrotomy. Damage from the process is visible, but individual crystals are still observable within the grain. The X grains were composed of many small crystal domains (Fig. 3), ranging in size from 24 – 296 nm in diameter. Six of the X grains were composed of similarly sized crystals (median diameter of 140 nm), while one X grain contained much smaller crystals (median diameter of 51 nm). The small crystal sizes were similar to those previously observed in X grains [7]. X grain crystal sizes are markedly different from those of mainstream grains. Both mainstream grains were composed of a few large crystals (0.5 – 1.7 µm in diameter) (Fig. 4). In previous TEM work on smaller mainstream grains, the observed grains were composed primarily of single crystals 0.18 – 0.39 µm in diameter [5]. However, because some SiC properties have been observed to vary with grain size [11, 13], it was important to compare the X grains to similarly sized mainstream grains. By comparing both mainstream and X grains from the same size fraction, it is clear that the difference in crystal size is likely a result of formation timescales due to the differing stellar environments. Calculations based on stellar models, kinematical constraints, and equilibrium thermodynamics predict that mainstream grains form in AGB outflows over a period of years [14], whereas isotopic evidence for the incorporation of live ^{49}V (half life = 338 days) into SiC X grains suggests that X grains must condense in SNe outflows over a timescale of months [4]. TEM observations agree with the idea of rapid formation of SiC X grains, resulting in small crystal domains.

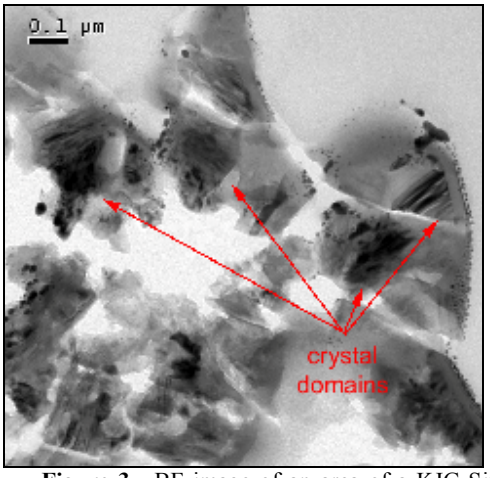

Figure 3. BF image of an area of a KJG SiC X grain. Multiple crystal domains (arrows) are visible within the grain. Intensity variations between domains are due to orientation-dependent diffraction contrast.

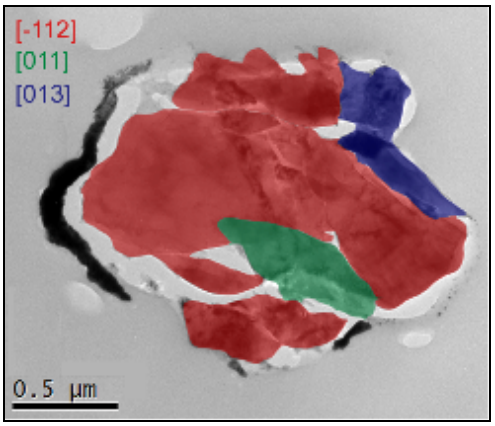

Figure 4. BF image of a KJG mainstream grain with a false-color overlay showing the three crystal domains in the grain and the nearest zone axis parallel to the TEM beam.

Previous observations of mainstream grains have found only the two lowest formation temperature polytypes present in presolar SiC: 3C-SiC (cubic: a = 4.36 Å; 79% by number observed by [5]) and 2H-SiC (hexagonal: a = 3.08 Å, c = 5.03 Å; 3%) [5]. An intergrowth between the two polytypes (17%) and a small number of 1-D disordered grains (1%) have also been observed. In this study, microdiffraction patterns were obtained for both mainstream grains and from several crystal domains in each X grain, and the polytype was determined, mainly from <110> zones. Both mainstream grains were consistent with the 3C-SiC polytype, as were most of the X grains. Also observed was one case of an intergrowth between the 3C-SiC and 2H-SiC polytypes and one disordered crystal. Twinning occurred frequently in both the mainstream and X grains. Polytypes are extremely sensitive to physical conditions, such as temperature and pressure, during grain formation. Despite condensation in different environments, mainstream grains and X grains appear to form the same polytypes. However, because higher densities exist in SN outflows, it is possible that higher-order hexagonal and rhombohedral polytypes could exist in X grains, though none have yet been observed.

Acknowledgements: We thank Roy Lewis (Enrico Fermi Institute/University of Chicago) for providing the Murchison KJG samples.

References: [1] Meyer B.S. and Zinner E., in *MESS II* Lauretta D. S., McSween H. Y., Jr., Eds. (Univ. of Arizona, Tucson, 2006) pp. 69-108. [2] Amari S. et al. (1992) *ApJ* 394, L43. [3] Nittler L.R. et al. (1996) *ApJ* 462, L31. [4] Hoppe P. and Besmehn A. (2002) *ApJ* 576, L69. [5] Daulton T.L. et al. (2003) *GCA* 67, 4743. [6] Daulton T.L. et al. (2006) *Met. Planet. Sci.* 41, A42. [7] Stroud R.M. et al. (2004) *Met. Planet. Sci.* 39, A101. [8] Amari S. et al. (1994) *GCA* 58, 459. [9] Nittler L.R. et al. (1995) *ApJ* 453, L25. [10] Zinner E. et al. (2007) *GCA* 71, 4786. [11] Amari S. et al. (1995) *Meteoritics* 30, 679. [12] Hynes K.M. and Gyngard F.M. (2009) *LPSC* XXXX, Abstract #1198 http://presolar.wustl.edu/~pgd. [13] Hoppe P. et al. (1996) *GCA* 60, 883. [14] Bernatowicz T.J. et al. (2005) *ApJ* 631, 988.